THE JOURNAL OF BIOLOGICAL CHEMISTRY VOL. 283, NO. 19, pp. 13108–13115, May 9, 2008

CD36 Mediates Both Cellular Uptake of Very Long Chain Fatty Acids and Their Intestinal Absorption in Mice*[S]

Received for publication, September 27, 2007, and in revised form, February 22, 2008 Published, JBC Papers in Press, March 10, 2008, DOI 10.1074/jbc.M708086200

Victor A. Drover[‡1,2], David V. Nguyen[§], Claire C. Bastie[‡], Yolanda F. Darlington[‡3], Nada A. Abumrad[¶], Jeffrey E. Pessin[‡], Erwin London[‖], Daisy Sahoo[‡1], and Michael C. Phillips[§]

From the Departments of [‡]Pharmacology and [‖]Biochemistry and Cell Biology, State University of New York, Stony Brook, New York 11794, the [§]GI/Nutrition Division, The Children's Hospital of Philadelphia, University of Pennsylvania School of Medicine, Philadelphia, Pennsylvania 19104, and the [¶]Department of Medicine, Washington University School of Medicine, St. Louis, Missouri 63110

The intestine has an extraordinary capacity for fatty acid (FA) absorption. Numerous candidates for a protein-mediated mechanism of dietary FA absorption have been proposed, but firm evidence for this process has remained elusive. Here we show that the scavenger receptor CD36 is required both for the uptake of very long chain FAs (VLCFAs) in cultured cells and the absorption of dietary VLCFAs in mice. We found that the fraction of CD36-dependent saturated fatty acid association/absorption in these model systems is proportional to the FA chain length and specific for fatty acids and fatty alcohols containing very long saturated acyl chains. Moreover, intestinal VLCFA absorption is completely abolished in CD36-null mice fed a high fat diet, illustrating that the predominant mechanism for VLCFA absorption is CD36-dependent. Together, these findings represent the first direct evidence for protein-facilitated FA absorption in the intestine and identify a novel therapeutic target for the treatment of diseases characterized by elevated VLCFA levels.

In typical Western diets, the bulk of the calories exist in the chemical form of triacylglycerols (TAGs)[4] that consist of glycerol esterified to three fatty acid (FA) molecules. Once consumed, the FAs are liberated from TAG via pancreatic enzymes and are quantitatively absorbed by the body for energy, storage, and other cellular processes. The mechanism(s) responsible for the absorption of dietary FAs have not been well characterized. Given the extraordinary capacity of the gut for FA absorption, it seems likely that diffusion plays a major role in this process. The most common fatty acids in a typical diet are the long chain FAs palmitate (16:0) and oleate (18:1), which have relatively high rates of simple diffusion in model membrane systems (reviewed in Ref. 1).

Unlike the long chain FAs, saturated very long chain FAs (VLCFAs) are much less soluble in aqueous environments, and the diffusion rates are much lower. In mixtures of vesicles and albumin (which model FA delivery to peripheral cells such as adipocytes), VLCFAs partition more favorably into phospholipid bilayers compared with long chain FAs (2). In addition, the dissociation of saturated VLCFAs from model vesicles is 10^5–10^6-fold slower than the dissociation of long chain FAs (3). This combination of preferential partitioning and slow dissociation suggests that protein-based mechanisms may be required for efficient absorption and utilization of VLCFAs in peripheral tissues *in vivo*.

In contrast to peripheral absorption, VLCFA absorption in the intestine is essentially an unstudied field. The only direct experimentation to date was published in 1963 wherein Fields and Gatt (4) determined that intragastric or intraduodenal [^{14}C]lignoceric acid (24:0) was absorbed in the rat intestine and appeared in the lymph primarily in the neutral glyceride fraction (*i.e.* triacylglycerol). Since then, intestinal fatty acid absorption has been primarily studied using only long chain FAs and often employed indirect measures such as the appearance of radiolabeled FAs in the blood following inhibition of lipases with detergent.

In the current study, we explored the mechanisms of intestinal VLCFA absorption. We hypothesized that the relatively high diffusion rates of long chain FAs in the gut might obscure the detection of protein-facilitated processes and thus exploited the much lower diffusion rates of VLCFAs to circumvent this problem. As a candidate facilitator of FA absorption, we chose CD36, an 88 kDa, multiligand scavenger receptor strongly implicated in intestinal FA utilization. CD36 is expressed in epithelial cells of the small intestine along the gastro-colic and crypt-to-villus axes in a pattern paralleling that of other proteins implicated in FA uptake such as intestinal and liver FA-binding proteins (5–7). In addition, we have shown that CD36 is important for chylomicron production and acute FA uptake in the proximal intestine (8, 9).

* This work was supported, in whole or in part, by National Institutes of Health Grants DK060022 (to N. A. A.), HL22633 (to M. C. P.), and HL63768 (to E. L.). The costs of publication of this article were defrayed in part by the payment of page charges. This article must therefore be hereby marked "*advertisement*" in accordance with 18 U.S.C. Section 1734 solely to indicate this fact.

[S] The on-line version of this article (available at http://www.jbc.org) contains supplemental Fig. S1.

[1] Current address: Dept. of Medicine, Medical College of Wisconsin, 8701 Watertown Plank Rd., Milwaukee, WI 53226.

[2] To whom correspondence should be addressed: H4880 Health Research Center, 8701 Watertown Plank Rd., Milwaukee, WI 53089. Tel.: 414-456-4607; Fax: 414-456-6570; E-mail: victor.drover@mcw.edu.

[3] Current address: Baylor College of Medicine, One Baylor Plaza, Houston, TX 77030.

[4] The abbreviations used are: TAG, triacylglycerol; 2-MAG, 2-monoacylglycerol; CE, cholesteryl ester; COE, cholesteryl oleoyl ether; *E*, absorption efficiency; FA, fatty acid; HFHC, high fat high cholesterol; NPC1L1, Niemann-Pick C1-like 1 protein; POPC, 1-palmitoyl-2-oleoyl-*sn*-glycero-3-phosphocholine; TCA, taurocholate; V, velocity; VLCFA, very long chain fatty acid; X-ALD, X-linked adrenoleukodystrophy; PBS, phosphate-buffered saline; WT, wild type; HDL, high density lipoprotein.

As described herein, we explored the mechanisms of intestinal FA absorption in COS7 cells using a novel bile salt-based assay. Complementary *in vivo* studies of intestinal VLCFA absorption were also performed using the fecal dual isotope recovery method in WT, CD36-deficient, and SR-BI-deficient mice fed either chow or a high fat, high cholesterol (HFHC) diet. The data show for the first time that the mechanism of dietary VLCFA transfer into the brush border membrane of enterocytes is primarily protein-mediated.

EXPERIMENTAL PROCEDURES

Preparation and Characterization of Lipid/Bile Salt Particles—Particles were prepared by drying down under $N_{2(g)}$ 0.38 mg of 1-palmitoyl-2-oleoyl-*sn*-glycero-3-phosphocholine (POPC), 0.02 mg of cholesterol, and trace amounts of ^{14}C- or ^{3}H-labeled lipids. Samples were resuspended in 10 ml of PBS containing, unless otherwise stated, 5 mM taurocholate (TCA, pH 7.4) with gentle rocking at ambient temperature. The following radiolabeled ^{14}C-labeled FAs (American Radiolabeled Chemicals, Inc., St. Louis, MO; 50–60 mCi/mmol) were used: palmitic acid (16:0), stearic acid (18:0), arachidic acid (20:0), behenic acid (22:0), docosahexaenoic acid (22:6n-3), lignoceric acid (24:0), hexacosanoic acid (26:0), lignoceryl alcohol (24:0-ol), taurocholic acid, 1-palmitoyl-2-oleoyl-*sn*-glycero-3-phosphocholine, cholesterol, sitostanol, and cholesteryl oleate. [^{3}H]Cholesteryl oleoyl ether (American Radiolabeled Chemicals) and [^{14}C]glucose 6-phosphate (PerkinElmer) were also used. Where indicated, an unlabeled competitor (16:0, 24:0, or 2-monoacylglycerol) was dried down with the lipids prior to resuspension in TCA.

To analyze the association of lipids with mixed micelles, particles prepared with 5 mM TCA and ^{14}C-labeled 16:0, 24:0, glucose 6-phosphate, or cholesterol were separated from the bulk aqueous phase (marked by [^{14}C]glucose 6-phosphate) by gravity gel filtration though Sephadex G25 equilibrated in 5 mM TCA.

Measuring Cell-associated ^{14}C and ^{3}H Lipid Levels in Vitro—COS7 cells were maintained in Dulbecco's modified Eagle's medium containing 10% calf serum, 2 mM L-glutamine, 50 units/ml penicillin, 50 μg/ml streptomycin, and 1 mM sodium pyruvate. Cells at 80% confluence in 100-mm dishes were transfected with FuGENE 6 (Roche Applied Sciences, Indianapolis, IN) and 10 μg of the indicated vector unless otherwise indicated (see Fig. 3*A*). Previously described pSG5-based expression vectors encoding native and chimeric scavenger receptors (pSG5(rCD36) (10); pSG5(mSR-BI) (11), pSG5(SR/CD/SR) (11); pSG5(CD/SR/CD) (12); see also Fig. 5*A*) were used to transfect COS7 cells.

Twenty-four hours post-transfection, cells were passaged, pooled when multiple plates were transfected with the same vector, and re-plated into 12-well culture dishes. 48-h post-transfection, cells were washed twice with PBS (ambient temperature) and incubated with 1 ml of lipid/bile salt micelles containing 100,000 dpm of the indicated ^{14}C- or ^{3}H-labeled lipids for 3 min unless otherwise specified. The cells were then washed three times with PBS and dried for 5 min. The associated radioactivity was determined in isopropyl alcohol lipid extracts by liquid scintillation spectrometry and expressed relative to cellular protein levels as described previously (13). Data are expressed as either the fractional uptake (the percentage of the total radioactivity applied to the cells which remains cell-associated following three washes with PBS) or normalized to total cellular protein levels and expressed as the velocity of uptake (nmol of substrate that remain cell-associated following three washes with PBS divided by the total time of incubation). In each case, cell-associated radioactivity includes any radioactivity internalized by the cell and any remaining on the cell surface. HDL binding to COS7 cells was measured as previously described (11).

Mouse Genotyping and Characterization—CD36$^{-/-}$ and SR-BI$^{-/-}$ mice backcrossed to the C57BL6/J background were used to produce CD36$^{-/-}$SR-BI$^{-/-}$ double knock-out mice by selective husbandry of F_1 (CD36$^{+/-}$SR-BI$^{+/-}$) littermates. Mouse genotyping was performed by PCR using primers specific for the WT and null alleles of CD36 and SR-BI. The sequences of the CD36 screening primers are: 5′-CCG CTT CCT CGT GCT TTA CGG TAT C; 5′-GGT ACA ATC ACA GTG TTT TCT ACG TGG; 5′-CAG CTC ATA CAT TGC TGT TTA TGC ATG. The sequences of the SR-BI screening primers are: 5′-AGT CTC GGC TTC TGT CAT CTC T; 5′-GTC AGT CAA ACC CTG TGA CAA C; 5′-AGG TGA GAT GAC AGG AGA TC. Genotypes were confirmed by protein immunoblotting using antibodies specific for CD36 (Cascade Biosciences, Winchester, MA), and SR-BI (Novus Biologicals, Littleton, CO); anti-p115 (BD Biosciences, San Jose, CA) was used as a loading control for protein immunoblotting. These primary antibody:epitope complexes were detected using the appropriate horseradish peroxidase-conjugated secondary antibodies followed by luminol-based chemiluminescent signal capture on photographic film.

Analysis of cholesterol and FA mass in plasma from fasted mice (12 h) was performed using standard chemistries (Infinity Cholesterol, Thermo Electron Corp., Melbourne, Australia; free fatty acids half micro test, Roche Applied Sciences). Plasma cholesterol profiles were obtained using the reagent described above following Sepharose 6 fractionation of plasma.

Intestinal Absorption Efficiency—The fecal dual isotope recovery method (14) relies on the inability of mice to efficiently absorb the plant sterol [5,6-^{3}H]-$\alpha\beta$-sitostanol. When given via intragastric gavage to mice, the majority of the sitostanol radioactivity can be recovered from a 24-h collection of the feces. After co-administering a bolus of a ^{14}C-labeled substrate with the sitostanol in corn oil and collecting feces for 24 h, the absorption efficiency (*E*) of the unknown was determined by Equation 1,

$$E = [(R_i - R_f)/R_i] \times 100 \quad \text{(Eq. 1)}$$

where R_i is the ^{14}C/^{3}H ratio in the administered bolus, and R_f is the ^{14}C/^{3}H ratio in fecal lipid extracts. Ratios of ^{14}C/^{3}H were determined empirically using scintillation spectrometry. When ezetimibe was used as an inhibitor, the appropriate amount (10 mg/kg body weight) was dissolved in 0.15 ml of corn oil and administered by gavage to the mice 30 min before the gavage of corn oil containing the radioactive lipids.

Statistics—Data shown represent the means ± S.E., and all *in vitro* analyses are representative of at least two independent

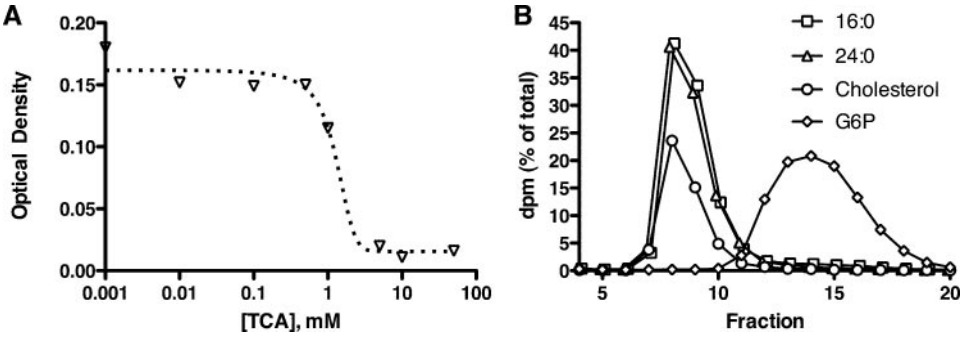

FIGURE 1. **Lipid solubilization by TCA.** *A*, lipid solubilization by bile salt. POPC and cholesterol were dried down and resuspended in a solution of TCA. Micelle formation was assessed by reduced turbidity (optical density at 560 nm) as a function of TCA concentration. *B*, micelle fractionation. Micelles were prepared in 5 mM TCA in the presence of trace amounts of radiolabeled 16:0, 24:0, cholesterol, or glucose 6-phosphate (*G6P*) and fractionated by size exclusion chromatography through a Sephadex G25 resin (3.7-ml column volume, 13-cm column height, 0.25 ml fraction size) equilibrated in 5 mM TCA. The data are displayed as dpm in each fraction expressed as a percentage of the total dpms applied to the column. The 16:0 and 24:0 traces have been displaced by 0.1 fractions to the *right* and *left*, respectively, to improve visibility.

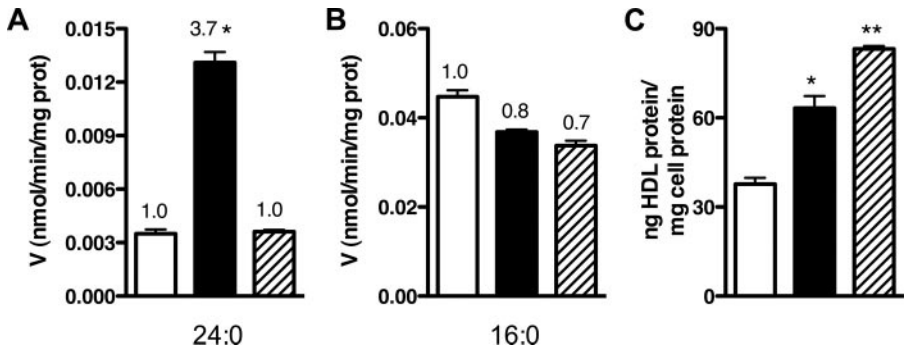

FIGURE 2. **CD36 mediates the uptake of lignocerate in COS7 cells.** *A* and *B*, fatty acid uptake. The average velocity (*V*) of [^{14}C]24:0 (*A*) and [^{14}C]16:0 (*B*) association was determined in COS7 cells transfected with a control vector (*open bars*), pSG5(rCD36) (*filled bars*), or pSG5(mSR-BI) (*hatched bars*) using a 3-min incubation time. Data are expressed as nmol of FA associated with the cells per minute and normalized to cellular protein mass. Fold changes relative to control vector are indicated *above* the bars and show a significant effect of CD36 on cell-associated 24:0. *, $p < 0.001$, $n = 4$. *C*, receptor expression on the cell surface. Cell surface receptor expression as determined by measuring HDL binding in COS7 cells transfected with a control vector (*open bar*), pSG5(rCD36) (*filled bar*), or pSG5(mSR-BI) (*hatched bar*). *, $p < 0.01$; **, $p < 0.001$, $n = 4$.

experiments. Differences were evaluated using one-way or two-way analysis of variance as appropriate, and *p* values for individual comparisons were determined using Bonferonni post-tests. Linear regression (Fig. 3, *B* and *C* only) was evaluated using the Pearson product moment, *r*. Analysis of co-variance (Fig. 3*B* only) was used to test differences in the uptake rate (*i.e.* slope) over time. Significant differences are indicated in the figures with an asterisk; *p* values and sample size (*n*) are noted in the figure legends.

RESULTS

CD36 Mediates Cellular VLCFA Association from Bile Salt-containing Lipid Particles—In the intestinal lumen, FAs and other lipids are emulsified by phospholipids and bile salts. To mimic this essentially protein-free FA delivery system, we prepared mixed lipid/bile salt particles composed of TCA, POPC (0.5 mM), and cholesterol (0.05 mM). Mixed micelle formation over a range of TCA concentrations was monitored by the loss of light scattering at 560 nm; TCA concentrations of 5 mM and higher were sufficient to dissolve the lipids (Fig. 1*A*). When mixtures of POPC, cholesterol, and TCA were prepared in the presence of trace amounts of [^{14}C]lignocerate (24:0) or [^{14}C]palmitate (16:0), greater than 99% of the detectable radioactivity eluted as a single peak that co-eluted with cholesterol when chromatographed by gravity gel filtration through Sephadex G-25 using a TCA-containing buffer (Fig. 1*B*). This shows that both long chain (16:0) and very long chain (24:0) FAs were incorporated into the micellar particles. That each fatty acid co-eluted with cholesterol indicated that the particles formed could accommodate lipids of various chain lengths and hydrophobicities. These particles were clearly larger than glucose 6-phosphate, which eluted as a unique, smaller peak. Chromatography through Superose 6 gave similar results and showed that POPC co-eluted with the cholesterol and FA, at approximately double the void volume (data not shown). These experiments indicated that the POPC, cholesterol, and FA that had dissolved in the TCA had formed mixed micellar particles. These lipid/bile salt particles were used to model intestinal FA uptake in cell-based assays.

To examine the role of CD36 in intestinal FA uptake, we added lipid/bile salt particles to COS7 cells transfected with a vector encoding CD36 (pSG5(rCD36); see Fig. 5*A*) and measured the velocity of [^{14}C] association with the cells. As shown in Fig. 2*A*, COS7 cells expressing CD36 (*filled bar*) exhibited a 3.7-fold higher average velocity (*V*) of 24:0 association ($V_{24:0}$) compared with mock-transfected controls (*open bars*). No significant enhancement was noted for $V_{16:0}$ in cells expressing CD36 (Fig. 2*B*, *filled bar*). Expression of a different class B scavenger receptor, the HDL receptor SR-BI encoded by pSG5(mSR-BI), had no significant effect on either $V_{24:0}$ or $V_{16:0}$ (Fig. 2, *hatched bars*), even though SR-BI is also implicated in intestinal fat absorption/processing (15, 16) and is structurally related to CD36. To control for scavenger receptor-dependent differences in cell surface expression, we measured HDL binding in cells transfected with either CD36 or SR-BI. Compared with mock-transfected controls we observed a similar increase in HDL binding in cells transfected with CD36 and SR-BI (Fig. 2*C*) indicating similar expression levels of the scavenger receptors.

CD36-mediated VLCFA Association Is a Saturable Process Specific for Saturated, Very Long Acyl Chains—To further characterize CD36-dependent effects on FA association *in vitro*, we used cells transfected with varying amounts of pSG5(rCD36) to titrate CD36 expression. Protein immuno-

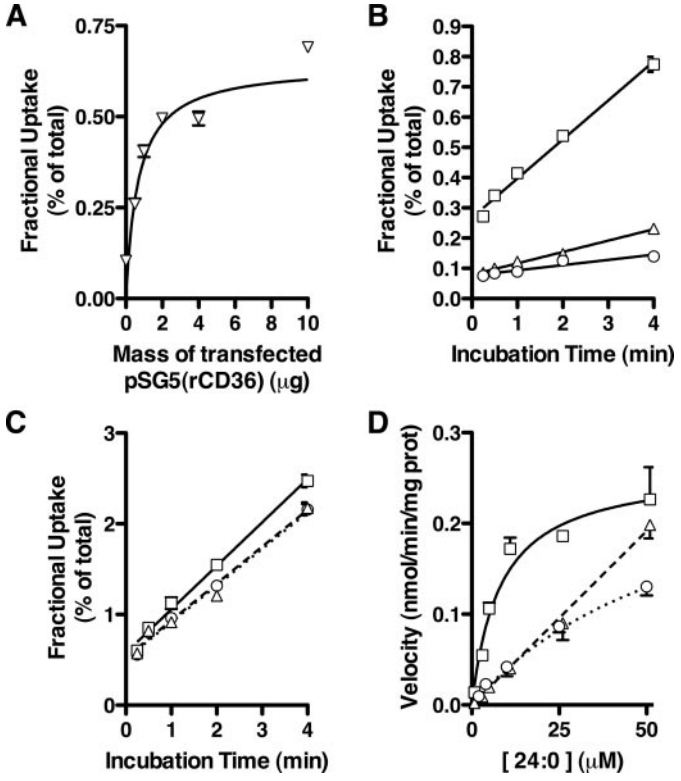

FIGURE 3. **Properties of CD36-mediated 24:0 uptake.** *A*, receptor dose dependence. Fractional uptake of [^{14}C]24:0 was determined in COS7 cells transfected with increasing amounts of pSG5(rCD36). Data are expressed as the percentage of total radioactivity added to the cells ($n = 4$). *B* and *C*, fractional uptake of FAs over time. Fractional uptake of [^{14}C]24:0 (*B*) and [^{14}C]16:0 (*C*) in COS7 cells was measured over time following transfection with a control vector (*open circles*), pSG5(rCD36) (*open squares*), or pSG5(mSR-BI) (*open triangles*). Data are expressed as the percentage of total radioactivity added to the cells. A linear relationship was observed between 0.25 and 4 min of [^{14}C]24:0 incubation for each data set ($r \geq 0.9530$, $0.0003 \leq p \leq 0.0121$, $n = 4$). *D*, velocity of 24:0 uptake with increasing substrate concentration. The velocity of [^{14}C]24:0 uptake in COS7 cells ($n = 4$) was measured in the presence of increasing 24:0 concentration following transfection with a control vector (*open circles*), pSG5(rCD36) (*open squares*), or pSG5(mSR-BI) (*open triangles*).

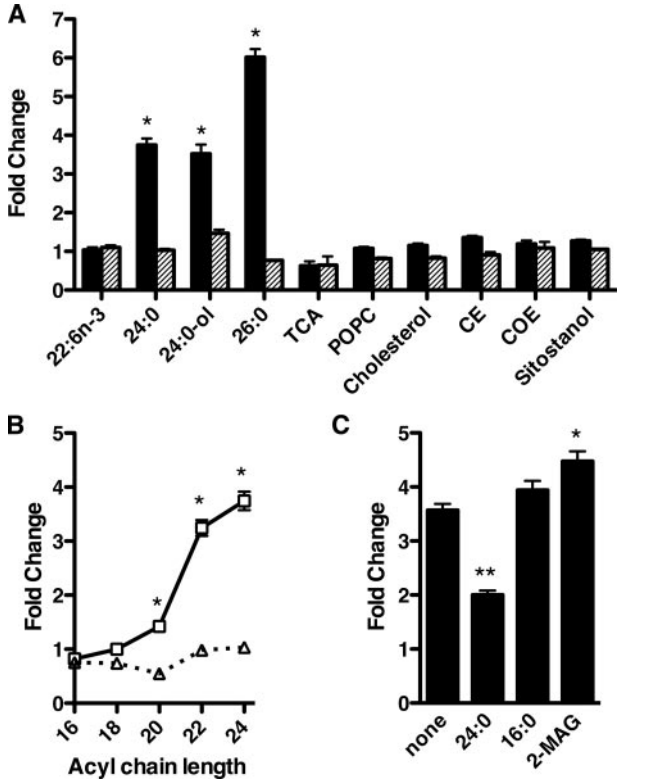

FIGURE 4. **CD36-dependent selective association of very long chain fatty acids and fatty alcohols with COS7 cells.** *A*, ligand specificity of CD36-dependent uptake. The velocity of uptake of various radioactive lipids was determined in 3 min in COS7 cells transfected with pSG5(rCD36) (*closed bars*) or pSG5(mSR-BI) (*hatched bars*) and expressed as a fold change compared with a mock-transfected control (fold-change = 1). The following lipids were used: docosahexaenoate (22:6n-3), lignocerate (24:0), lignoceryl alcohol (24:0-ol), hexacosanoate (26:0), TCA, POPC, cholesterol, CE, COE, and sitostanol. *, $p < 0.0001$, $n = 4$. *B*, chain length specificity of CD36-dependent uptake. The effect of chain length on the velocity of saturated FA uptake was determined in COS7 cells transfected with pSG5(rCD36) (*open squares*) or pSG5(mSR-BI) (*open triangles*) and expressed as a fold change compared with a mock-transfected control (fold-change = 1). *, $p < 0.001$, $n = 4$. *C*, detecting CD36 ligands by competition. COS7 cells were transfected with pSG5(rCD36) and incubated with radiolabeled particles containing 50 μM of the indicated non-radioactive competitors. The velocity of uptake was measured as described above and expressed as fold-change over mock-transfected controls (fold-change = 1). *, $p < 0.05$; **, $p < 0.001$, $n = 4$.

blotting confirmed that this range of DNA mass produced a steady increase in CD36 protein mass under the transfection parameters described (see supplemental Fig. S1, *A* and *B*). The amount of 24:0 associated with COS7 cells as a percentage of total substrate (*i.e.* the fractional uptake) increased with the amount of pSG5(rCD36) used in the transfection until a saturating value was reached (Fig. 3*A*). The 24:0 fractional uptake correlated with cell surface CD36 expression ($r = 0.7650$, $p < 0.05$) as determined by HDL binding (see supplemental Fig. S1*C*).

The fractional uptake of 24:0 with COS7 cells also increased with the time of incubation when the mass of pSG5(rCD36) transfected was constant (Fig. 3*B*). The steady state rate of association (*i.e.* the slope of the line in Fig. 3*B*) in cells expressing CD36 (0.13 ± 0.006% of total dpm/min) is significantly faster than in either SR-BI-expressing (0.038 ± 0.002% of total/min, $p < 0.0001$, $n = 4$) or mock-transfected cells (0.017 ± 0.002% of total/min, $p < 0.0001$, $n = 4$). The steady state rate of association of 16:0 with the cells was only slightly increased by CD36 expression (Fig. 3*C*). We also measured the velocity of 24:0 association over a range of substrate concentrations. Fig. 3*D* illustrates that, as the concentration of 24:0 increases, the $V_{24:0}$ reaches a plateau ($V_{max} = 0.26 \pm 0.02$ nmol/min/mg, $K_m = 8.19 \pm 2.24$ μM) consistent with facilitated diffusion. In contrast, $V_{24:0}$ in mock-transfected cells increases essentially linearly with 24:0 concentration. This is the predicted behavior for a process mediated by simple diffusion.

To determine the substrate specificity of CD36-mediated lipid uptake, we performed assays in COS7 cells using a panel of lipids. Unlike the uptake of 24:0 and 26:0, the average velocity of cell association of the polyunsaturated FA docosahexaenoate (22:6n-3) was unaffected by either CD36 or SR-BI expression (Fig. 4*A*). A very long chain, saturated fatty alcohol (lignoceryl alcohol, 24:0-ol) displayed average velocities of CD36-dependent cell association comparable to 24:0 despite the substitution of a carboxylic acid group with an alcohol group.

In contrast to the results seen with the very long chain, saturated fatty acids and alcohols, the velocity of cellular association of TCA and POPC was unaffected by the expression of either

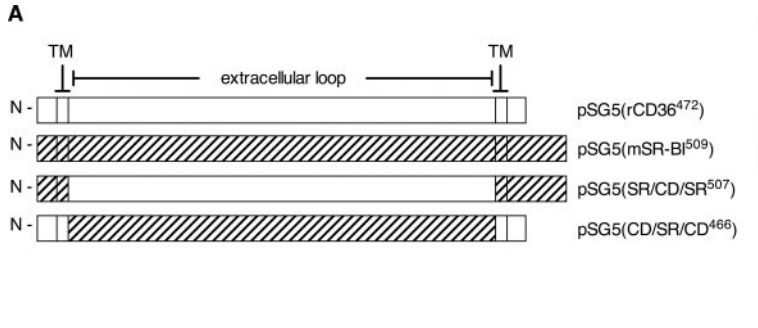

FIGURE 5. **Identifying the critical domains for CD36-dependent uptake of 24:0.** *A*, organization of cDNAs encoding CD36, SR-BI, and CD36-SR-BI chimeras. CD36 and SR-BI are predicted to have a hairpin topology with a large extracellular domain, 2 transmembrane domains (*TM*), and intracellular N/C termini. Complementary DNAs encoding CD36, SR-BI, and CD36-SR-BI chimeras were cloned into pSG5 and used to transfect COS7 cells. The predicted topology and organization of the cDNA for each construct is shown. CD36 fragments are indicated with *open bars*; SR-BI fragments are indicated with *hatched bars*. The number of amino acid residues in each construct is indicated numerically in the vector name. *B*, velocity of 24:0 uptake using CD36-SR-BI chimeras. The velocity of [^{14}C]24:0 uptake over 3 min was determined in COS7 cells transfected with the CD36-SR-BI receptor chimeras shown in *A*. Data are expressed as fold-change over mock-transfected controls (fold-change = 1). *, $p < 0.01$; **, $p < 0.001$, $n = 4$.

CD36 or SR-BI. We observed a similar lack of an effect of CD36 upon uptake with a variety of hydrophobic sterols and sterol derivatives including cholesterol, cholesteryl ester (CE), cholesteryl oleoyl ether (COE), and the plant sterol sitostanol. These data suggest that CD36 specifically increases the uptake of molecules containing a single very long, saturated acyl chain. To test this hypothesis, we repeated our assay using a series of saturated fatty acids with increasing chain length. We observed that the fold increase in the average velocity of FA association in cells expressing CD36 is directly related to the length of the acyl chain when the length of the FA backbone exceeds 18 carbon atoms (Fig. 4*B*). Expressing SR-BI in these cells had no significant effect on the amount of cell association for all of these FAs.

To further evaluate the specificity of CD36-facilitated VLCFA in our bile salt-based assay, we measured [^{14}C]24:0 uptake in the presence of high concentrations of unlabeled 24:0, 16:0, or 2-monoacylglycerol (2-MAG, the other hydrolytic product of TAG catabolism in the intestine). Under these conditions, ligands competing for CD36 would cause a reduction in the fractional uptake of [^{14}C]24:0. Only unlabeled 24:0 was able to compete for uptake of [^{14}C]24:0 in cells expressing CD36 (Fig. 4*C*). This result further supports the specificity of CD36 function in the cellular transfer of VLCFA and fatty alcohols from bile salt micelles.

The Extracellular Domain of CD36 Is Primarily Responsible for Cellular VLCFA Association—CD36 and SR-BI share a high degree of sequence similarity, but, as noted above, we found that SR-BI does not promote VLCFA absorption. Thus, we expressed chimeric CD36-SR-BI receptors (Fig. 5*A*) to determine the domains of CD36 responsible for facilitating 24:0 uptake. When we expressed the chimeric receptor consisting of the CD36 extracellular domain and the transmembrane domains/termini of SR-BI [pSG5(SR/CD/SR)] we detected a 4-to-5-fold increase in the velocity of 24:0 cellular association comparable to the native CD36. This suggests that the bulk of the facilitated VLCFA uptake is dependent upon the extracellular domain of CD36 (Fig. 5*B*). The complementary chimeric receptor containing the extracellular domain of SR-BI [pSG5(CD/SR/CD)] displayed a much smaller yet significant increase.

Mice Lacking CD36 and SR-BI Accumulate Cholesterol and FAs in the Plasma—Based on the data above, we predicted that CD36 would be responsible for VLCFA absorption from the diet. To test this prediction, we used mouse strains carrying a null allele at the CD36 locus. We also used SR-BI-deficient mice, as this strain displays elevated postprandial plasma TAG levels (15) and has thus been implicated in intestinal FA processing. Because both receptors have been suggested to cooperate in the uptake of dietary lipids (14, 17) we also used these mice to create a novel mouse strain containing homozygous-null alleles of both CD36 and SR-BI (CD36$^{-/-}$SR-BI$^{-/-}$). Genotypes in the parental mice as well as CD36$^{-/-}$SR-BI$^{-/-}$ mice were confirmed by PCR (data not shown) and protein immunoblotting (Fig. 6*A*). CD36$^{-/-}$SR-BI$^{-/-}$ mice were overtly normal in appearance and activity, exhibited a normal lifespan and were fertile when maintained on a diet enriched with probucol.

We also monitored the total plasma cholesterol and FA concentration in these mice to correlate the genotypes with the previously described phenotypes for the parental strains lacking SR-BI or CD36. Consistent with previous reports (18), both male and female mice lacking SR-BI (SR-BI$^{-/-}$ and CD36$^{-/-}$ SR-BI$^{-/-}$) exhibited a 2–3-fold increase in fasting plasma cholesterol levels compared with WT and CD36$^{-/-}$ mice (Fig. 6*B*). This increase was due primarily to an increase in HDL size as illustrated by a reduced HDL retention time when the plasma was fractionated by gel filtration (Fig. 7). Mice lacking both receptors also displayed a significant increase in plasma FA levels (Fig. 6*C*) although this was more prominent in female mice. Together, these data verify the successful production of a novel, pure-breeding mouse strain lacking both CD36 and SR-BI that exhibits the expected changes in plasma lipid levels. This new strain of mice along with the parental strains was used for all subsequent experiments.

CD36, but Not SR-BI or NPC1L1, Is Required for Efficient Intestinal Absorption of VLCFAs—Mice deficient in CD36 and/or SR-BI were used to test the role of these receptors in VLCFA uptake using the fecal dual isotope recovery method (14). This technique measures FA absorption efficiency (*E*) and, since it relies on the recovery of the substrate of interest from the feces, is arguably the best indicator of the total substrate absorption. As shown in Fig. 8*A*, deficiency of CD36 and/or SR-BI had no effect on the net absorption of 16:0 ($E_{16:0}$) in mice fed either a chow diet (*filled bars*) or a high fat, high cholesterol diet (*open bars*). The absorption of oleate (18:1) was similarly unaffected by scavenger receptor deficiency (data not shown). In contrast, CD36 deficiency, but not SR-BI deficiency, reduced $E_{24:0}$ by 73% on a basal diet (Fig. 8*B*, *filled bars*). When the mice

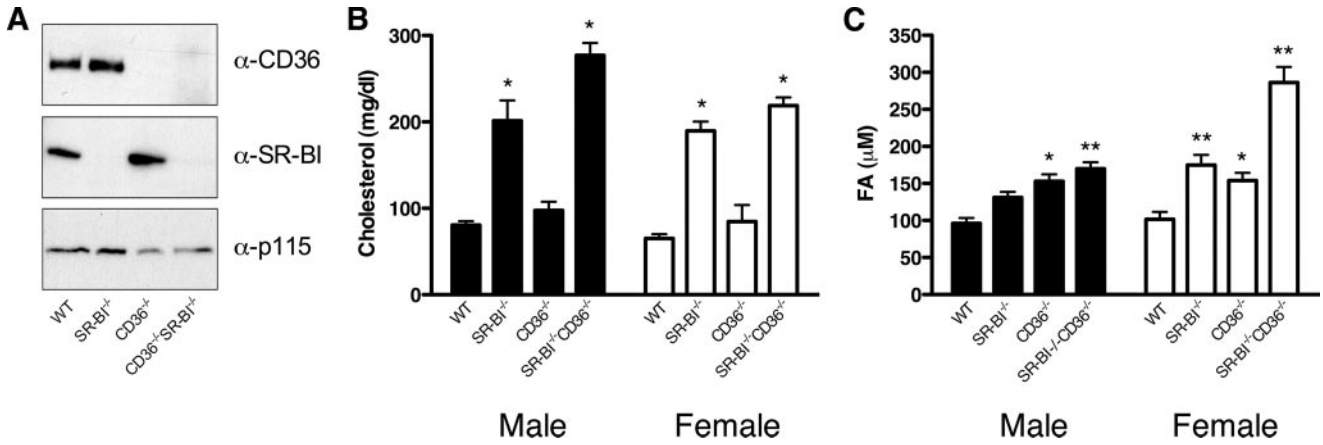

FIGURE 6. **Characterization of CD36- and SR-BI-deficient mice.** Mice deficient in either CD36 or SR-BI were crossed to produce a novel strain lacking both receptors. *A*, confirmation of receptor deficiency. Genotypes were verified by immunoblotting of adipose tissue protein extracts with α-CD36 and α-SR-BI antibodies. p115 was used as a loading control. *B* and *C*, effects of receptor deficiency on plasma lipid levels. Male (*closed bars*) and female (*open bars*) mice ($5 \leq n \leq 8$) of the indicated genotypes were fasted overnight, and the plasma levels of total cholesterol (*B*; *, $p < 0.001$) and total fatty acids (*C*; *, $p < 0.01$; **, $p < 0.001$) determined.

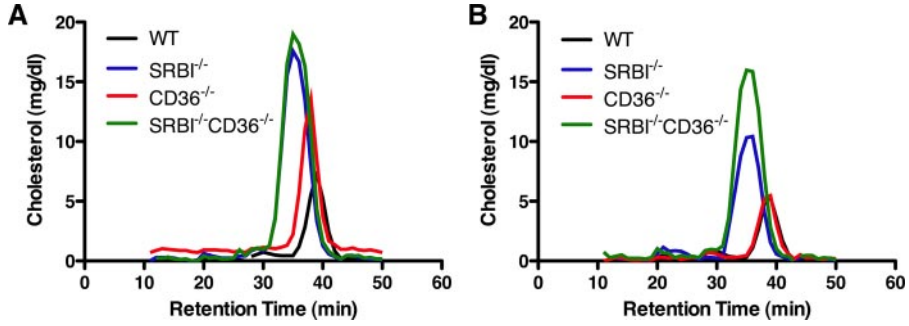

FIGURE 7. **Plasma cholesterol profiles in receptor-deficient mice.** *A* and *B*, plasma from fasting male (*A*) and female (*B*) mice was fractionated by size exclusion chromatography, and the cholesterol concentration in each fraction measured.

were placed on a HFHC diet (*open bars*), $E_{24:0}$ was extremely low (1.3 ± 1.8%). $E_{24:0}$ in CD36$^{-/-}$SR-BI$^{-/-}$ mice was comparable to CD36$^{-/-}$ regardless of diet. Because the HFHC diet did not significantly reduce $E_{24:0}$ in WT or SR-BI$^{-/-}$ mice, these data strongly indicate that CD36 plays an especially critical role in the uptake of VLCFAs under Western diet conditions.

We next extended our analysis to saturated FAs with varying chain lengths. Paralleling our observations in cultured cells (Fig. 4*B*), when animals were maintained on a HFHC diet facilitation of FA absorption by CD36 (given by the difference in *E* between WT and CD36$^{-/-}$ mice) was chain length-dependent, being detectable only with 20:0, 22:0, 24:0, and 26:0 FAs (Fig. 8*C*). The absolute efficiency of VLCFA uptake in WT mice was also chain length-dependent, but comparable decreases in *E* occurred with FAs that were 4 carbon atoms longer for WT than for CD36$^{-/-}$ mice.

Niemann-Pick C1 Like 1 (NPC1L1) is a protein required for the efficient absorption of dietary cholesterol in the intestine (19) and may act in a complex with other proteins such as SR-BI (20). In addition, NPC1L1 protein levels are dramatically elevated in the intestine of CD36-deficient mice (21). To determine if NPC1L1 may also be required for CD36-mediated VLCFA absorption, WT mice were treated with an oral dose of ezetimibe (10 mg/kg body weight), a specific inhibitor of NPC1L1-mediated cholesterol absorption (22), and $E_{24:0}$ measured as described above. In untreated and ezetimibe-treated mice, $E_{24:0}$ was comparable (control, 65.2 ± 11.7% *versus* ezetimibe-treated, 64.3 ± 11.7%, $n = 3$, $p > 0.05$) under conditions where cholesterol uptake was inhibited (14), indicating that NPC1L1 is not a critical component of the CD36-dependent VLCFA uptake pathway.

DISCUSSION

The exact role played by proteins participating in facilitated fatty acid transport remains controversial (reviewed in Ref. 23). Much of this debate is fuelled by the fact that many of the common fatty acids such as 16:0 and 18:1 have relatively high diffusion rates (compared with VLCFAs), which can mask facilitated processes (24). In the current report, we show that CD36 (but not the related scavenger receptor SR-BI) specifically facilitates the association of VLCFAs with transfected cells. This association exhibits saturable kinetics in the presence of excess substrate (a hallmark feature of a protein-mediated process), is chain length-dependent and correlates to the amount of CD36 expressed on the cell surface. In mice, we found that efficient VLCFA absorption required CD36 and observed chain length dependence similar to that seen using our cell-based assay. Together, the *in vitro* and *in vivo* data describe for the first time a protein-mediated pathway for VLCFA absorption in the intestine. To our knowledge, the CD36-deficient mouse is the first viable rodent model exhibiting reduced net absorption of dietary FA.

Similar to CD36, SR-BI is a class B scavenger receptor expressed on the plasma membrane of cells. Thus, we used SR-BI as a control receptor in our study to evaluate the specificity of CD36-dependent VLCFA cellular association. SR-BI had very little or no effect on VLCFA association in transfected COS7 cells. Our inability to detect an SR-BI-dependent effect was not due to reduced surface expression or altered subcellular distribution of the receptor as both CD36- and SR-BI-trans-

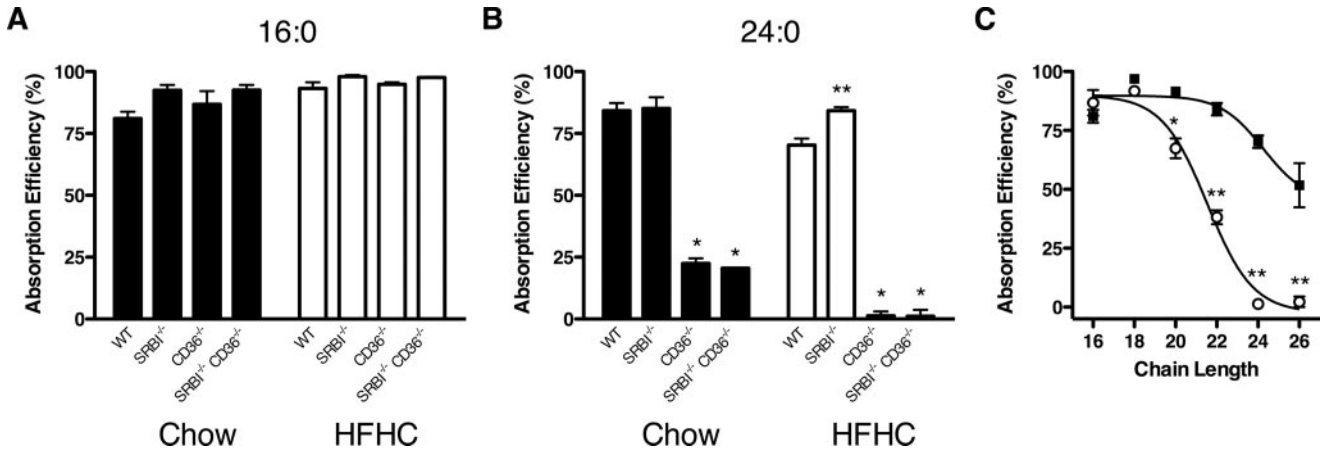

FIGURE 8. **FA absorption in receptor-deficient mice.** *A* and *B*, effect of HFHC diet on FA absorption. Absorption efficiency of orally administered [^{14}C]16:0 (*A*) and [^{14}C]24:0 (*B*) as measured in chow-fed (*filled bars*) and HFHC-fed (*open bars*) mice of the indicated genotypes using the fecal dual isotope recovery method. *, $p < 0.001$; **, $p < 0.01$, $n = 3$. *C*, chain length dependence of absorption efficiency. Absorption efficiency of a series of saturated fatty acids of the indicated chain length was measured in WT (*closed squares*) and CD36$^{-/-}$ (*open circles*) mice maintained on a HFHC diet. *, $p < 0.01$; **, $p < 0.001$, $n = 3$.

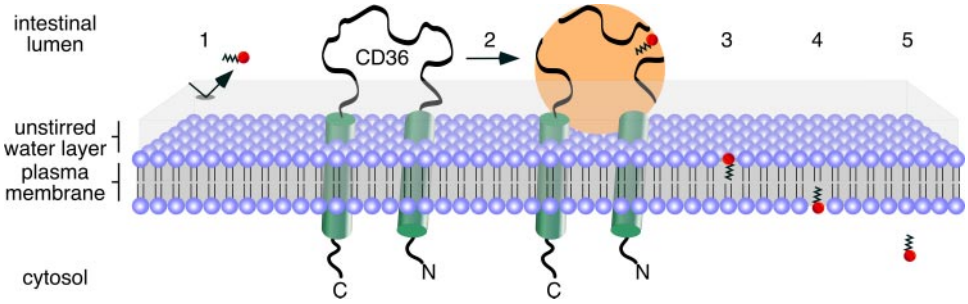

FIGURE 9. **Schematic illustration of CD36-mediated VLCFA absorption in the intestine.** VLCFAs are extremely hydrophobic and thus their passage through the aqueous unstirred water layer is lower (*1*) compared with long chain fatty acids such as palmitate and oleate. However, when packaged into bile salt and phospholipid-containing mixed micelles, VLCFAs can reach the plasma membrane of the enterocyte via the docking of the micelle to the extracellular domain of CD36 (*2*). By bringing the micelle and the plasma membrane into close proximity, the VLCFAs are transferred to the outer leaflet of the plasma membrane (*3*) following the concentration gradient. The VLCFAs can then flip to the inner leaflet of the plasma membrane (*4*) and then desorb to cytosolic fatty acid-binding proteins (*5*).

fected cells showed similar levels of HDL binding. This comparison is relevant for comparing the cell surface expression levels of the receptor because the binding affinity for HDL is similar for CD36 and SR-BI (11). We further supported this finding using a domain-swap experiment (Fig. 5) in which the extracellular domain of CD36 was shown to be required for the majority of the VLCFA absorption. Our animal data also agree with these *in vitro* findings as VLCFA absorption efficiency in SR-BI-deficient mice was comparable to that observed in WT mice. Together, the data allow us to conclude that the facilitation of VLCFA cellular association and intestinal absorption via CD36 is not a general property of class B scavenger receptors but rather is a specific property of CD36.

Because CD36 exhibits promiscuous ligand specificity and interacts with substrate-containing lipid particles (such as mixed micelles and lipoproteins, Ref. 25), we hypothesize that in the intestine, CD36 serves as a micelle docking protein. As VLCFA dissociation from the donor particle to the aqueous, unstirred water layer represents a major energy barrier, juxtaposing mixed bile salt/lipid micelles with the plasma membrane of enterocytes facilitates net VLCFA diffusion into the bilayer/cell. Thus, the proposed mechanism of CD36 action is to promote the direct transfer of 24:0 from the donor particle to the plasma membrane down a concentration gradient (Fig. 9). Because the extracellular domain of CD36 is predicted to protrude into the intestinal lumen, this is where we expect to find the domain(s) required for micelle docking. The results from our domain-swap experiment (Fig. 5) are consistent with this concept.

As noted earlier, VLCFAs preferentially partition into model membranes compared with long chain FAs (2). This may be sufficient to drive the differential CD36-facilitated uptake of long chain and very long chain FAs observed herein. The inability of 16:0 to compete for 24:0 cellular association in our *in vitro* assay (Fig. 4*C*) is also compatible with this model. However, we cannot rule out the possibility that CD36 directly binds long *versus* very long chain FAs via distinct binding sites or mechanisms and promotes their transfer to the membrane as has been previously suggested (1). Like albumin, CD36 may have unique binding sites for FAs of differing chain lengths (26).

We and others (8, 21, 27) have previously reported that the net absorption of long chain FAs is normal in CD36-deficient mice. Here, we confirm these data using the fecal dual isotope recovery method that is more precise than the indirect methods used previously. We utilized this technique to further show that the net absorption of long chain FAs in mice maintained on a high-fat diet is also normal. These data appear to contrast our recent finding that the intestinal absorption of 18:1 is delayed (but not reduced) in CD36-deficient mice following an acute, intragastric bolus of triacylglycerols enriched in triolein (21). The shorter time period (90 min) used in this triolein study *versus* 24 h for the fecal dual isotope recovery used in the present work is the primary difference likely leading to the disparate results. The acute TAG experiment indicated the existence of a compensatory effect on long chain FA absorption in distal seg-

ments of the intestine that apparently does not function for VLCFAs. This observation further underscores the notion that different mechanisms govern the absorption/utilization of long and very long chain dietary FAs. Additional experiments using FA:albumin complexes are required to determine if this difference is also present in peripheral tissues.

We have shown here that the net absorption of FAs is similarly unaffected by ezetimibe-inhibition of NPC1L1 or genetic SR-BI deficiency. These data are not consistent with the report of Bietrix *et al.* (15) suggesting that SR-BI does increase FA absorption. A number of methodological differences may account for this discrepancy. Firstly, Bietrix *et al.* monitored the plasma appearance of radiolabeled molecules in mouse plasma following an oral gavage of [^{14}C]cholesterol and [^{3}H]TAG (as opposed to free FAs as we have described here) in mice overexpressing SR-BI in the intestine and liver. This is an indirect technique that represents the sum of numerous metabolic processes including intestinal TAG lipolysis, FA absorption into enterocytes, secretion of newly synthesized TAG into the lymph and subsequent clearance from the plasma. The authors were careful to control for the latter by repeating the experiments following Triton WR1339 administration to inhibit lipase activity. However, the results could also be explained by increased enterocyte TAG secretion into lymph. As a cautionary example, CD36-deficient mice exhibit reduced lymph TAG secretion despite normal levels of FA absorption (8).

The data presented herein document for the first time a protein-mediated pathway for the absorption of dietary VLCFAs such as 24:0 and 26:0. These saturated FAs are the primary diagnostic metabolite in the debilitating disease X-linked adrenoleukodystrophy (X-ALD) and accumulate in the brain, adrenal gland, and blood as a result of mutations in the *ABCD1* gene (reviewed in Ref. 28). The function of ABCD1 is not known, and the mechanism of disease initiation remains uncertain. We speculate that CD36 is important for VLCFA uptake in the intestine and for transport from the blood into cells such as neurons and adrenocortical cells (Fig. 9). Importantly, CD36 mRNA levels are high in the adrenal (29) and brain (30). By inhibiting VLCFA uptake in these tissues, it may be possible to reduce cellular VLCFA levels, reduce symptoms of X-ALD, and/or delay the onset of the disease. Further study is warranted to assess the potential role of CD36 in the pathology of X-ALD.

Acknowledgments—We thank Elitza Ivanova and Cecil Hunter for technical support as well as Margery Connelly for providing the CD36-SR-BI chimeric constructs.

REFERENCES

1. Hamilton, J. A. (1998) *J. Lipid Res.* **39,** 467–481
2. Ho, J. K., Moser, H., Kishimoto, Y., and Hamilton, J. A. (1995) *J. Clin. Investig.* **96,** 1455–1463
3. Zhang, F., Kamp, F., and Hamilton, J. A. (1996) *Biochemistry* **35,** 16055–16060
4. Fields, M., and Gatt, S. (1963) *Nature* **198,** 994–995
5. Chen, M., Yang, Y., Braunstein, E., Georgeson, K. E., and Harmon, C. M. (2001) *Am. J. Physiol. Endocrinol. Metab.* **281,** E916–E923
6. Lobo, M. V., Huerta, L., Ruiz-Velasco, N., Teixeiro, E., de la Cueva, P., Celdran, A., Martin-Hidalgo, A., Vega, M. A., and Bragado, R. (2001) *J. Histochem. Cytochem.* **49,** 1253–1260
7. Poirier, H., Degrace, P., Niot, I., Bernard, A., and Besnard, P. (1996) *Eur. J. Biochem.* **238,** 368–373
8. Drover, V. A., Ajmal, M., Nassir, F., Davidson, N. O., Nauli, A. M., Sahoo, D., Tso, P., and Abumrad, N. A. (2005) *J. Clin. Investig.* **115,** 1290–1297
9. Nauli, A. M., Nassir, F., Zheng, S., Yang, Q., Lo, C. M., Vonlehmden, S. B., Lee, D., Jandacek, R. J., Abumrad, N. A., and Tso, P. (2006) *Gastroenterology* **131,** 1197–1207
10. Ibrahimi, A., Sfeir, Z., Magharaie, H., Amri, E. Z., Grimaldi, P., and Abumrad, N. A. (1996) *Proc. Natl. Acad. Sci. U. S. A.* **93,** 2646–2651
11. Connelly, M. A., Klein, S. M., Azhar, S., Abumrad, N. A., and Williams, D. L. (1999) *J. Biol. Chem.* **274,** 41–47
12. Connelly, M. A., de la Llera-Moya, M., Monzo, P., Yancey, P. G., Drazul, D., Stoudt, G., Fournier, N., Klein, S. M., Rothblat, G. H., and Williams, D. L. (2001) *Biochemistry* **40,** 5249–5259
13. Johnson, W. J., Bamberger, M. J., Latta, R. A., Rapp, P. E., Phillips, M. C., and Rothblat, G. H. (1986) *J. Biol. Chem.* **261,** 5766–5776
14. van Bennekum, A., Werder, M., Thuahnai, S. T., Han, C. H., Duong, P., Williams, D. L., Wettstein, P., Schulthess, G., Phillips, M. C., and Hauser, H. (2005) *Biochemistry* **44,** 4517–4525
15. Bietrix, F., Yan, D., Nauze, M., Rolland, C., Bertrand-Michel, J., Comera, C., Schaak, S., Barbaras, R., Groen, A. K., Perret, B., Terce, F., and Collet, X. (2006) *J. Biol. Chem.* **281,** 7214–7219
16. Out, R., Kruijt, J. K., Rensen, P. C., Hildebrand, R. B., de Vos, P., Van Eck, M., and Van Berkel, T. J. (2004) *J. Biol. Chem.* **279,** 18401–18406
17. Werder, M., Han, C. H., Wehrli, E., Bimmler, D., Schulthess, G., and Hauser, H. (2001) *Biochemistry* **40,** 11643–11650
18. Rigotti, A., Trigatti, B. L., Penman, M., Rayburn, H., Herz, J., and Krieger, M. (1997) *Proc. Natl. Acad. Sci. U. S. A.* **94,** 12610–12615
19. Altmann, S. W., Davis, H. R., Jr., Zhu, L. J., Yao, X., Hoos, L. M., Tetzloff, G., Iyer, S. P., Maguire, M., Golovko, A., Zeng, M., Wang, L., Murgolo, N., and Graziano, M. P. (2004) *Science* **303,** 1201–1204
20. Sane, A. T., Sinnett, D., Delvin, E., Bendayan, M., Marcil, V., Menard, D., Beaulieu, J. F., and Levy, E. (2006) *J. Lipid Res.* **47,** 2112–2120
21. Nassir, F., Wilson, B., Han, X., Gross, R. W., and Abumrad, N. A. (2007) *J. Biol. Chem.* **282,** 19493–19501
22. Garcia-Calvo, M., Lisnock, J., Bull, H. G., Hawes, B. E., Burnett, D. A., Braun, M. P., Crona, J. H., Davis, H. R., Jr., Dean, D. C., Detmers, P. A., Graziano, M. P., Hughes, M., Macintyre, D. E., Ogawa, A., O'Neill, K. A., Iyer, S. P., Shevell, D. E., Smith, M. M., Tang, Y. S., Makarewicz, A. M., Ujjainwalla, F., Altmann, S. W., Chapman, K. T., and Thornberry, N. A. (2005) *Proc. Natl. Acad. Sci. U. S. A.* **102,** 8132–8137
23. Kampf, J. P., and Kleinfeld, A. M. (2007) *Physiology* (*Bethesda*) **22,** 7–14
24. Kamp, F., and Hamilton, J. A. (2006) *Prostaglandins Leukot Essent Fatty Acids* **75,** 149–159
25. Calvo, D., Gomez-Coronado, D., Suarez, Y., Lasuncion, M. A., and Vega, M. A. (1998) *J. Lipid Res.* **39,** 777–788
26. Choi, J. K., Ho, J., Curry, S., Qin, D., Bittman, R., and Hamilton, J. A. (2002) *J. Lipid Res.* **43,** 1000–1010
27. Goudriaan, J. R., Dahlmans, V. E., Febbraio, M., Teusink, B., Romijn, J. A., Havekes, L. M., and Voshol, P. J. (2002) *Mol. Cell Biochem.* **239,** 199–202
28. Moser, H. W. (1997) *Brain* **120,** 1485–1508
29. Zhang, X., Fitzsimmons, R. L., Cleland, L. G., Ey, P. L., Zannettino, A. C., Farmer, E. A., Sincock, P., and Mayrhofer, G. (2003) *Lab. Investig.* **83,** 317–332
30. Coraci, I. S., Husemann, J., Berman, J. W., Hulette, C., Dufour, J. H., Campanella, G. K., Luster, A. D., Silverstein, S. C., and El-Khoury, J. B. (2002) *Am. J. Pathol.* **160,** 101–112